American Mineralogist, Volume 83, pages 1469–1481, 1998

# Iron sulfides from magnetotactic bacteria: Structure, composition, and phase transitions

MIHÁLY PÓSFAI,[1,*] PETER R. BUSECK,[1] DENNIS A. BAZYLINSKI,[2] AND RICHARD B. FRANKEL[3]

[1]Departments of Geology and Chemistry/Biochemistry, Arizona State University, Tempe, Arizona 85287, U.S.A.
[2]Department of Microbiology, Immunology and Preventive Medicine, Iowa State University, Ames, Iowa 50011, U.S.A.
[3]Department of Physics, Californa Polytechnic State University, San Luis Obispo, California 93407, U.S.A.

## ABSTRACT

Using transmission electron microscopy, we studied the structures and compositions of Fe sulfides within cells of magnetotactic bacteria that were collected from natural habitats. Ferrimagnetic greigite ($Fe_3S_4$) occurred in all types of sulfide-producing magnetotactic bacteria examined. Mackinawite (tetragonal FeS) and, tentatively, sphalerite-type cubic FeS were also identified. In contrast to earlier reports, we did not find pyrite ($FeS_2$) or pyrrhotite ($Fe_{1-x}S$). Mackinawite converted to greigite over time within the bacteria that were deposited on electron microscope grids and stored in air. Orientation relationships between the two minerals indicate that the cubic-close-packed S substructure remains unchanged during the transformation; only the Fe atoms rearrange. Neither mackinawite nor cubic FeS are magnetic, and yet they are aligned in chains such that when converted to magnetic greigite, the probable easy axis of magnetization, [100], is parallel to the chain direction. The resulting chains of greigite are ultimately responsible for the magnetic dipole moment of the cell. Both greigite and mackinawite magnetosomes can contain Cu, depending on the sampling locality. Because bacterial mackinawite and cubic FeS are unstable over time, only greigite crystals are potentially useful as geological biomarkers.

## INTRODUCTION

Magnetotactic bacteria synthesize membrane-bounded, intracellular, ferrimagnetic crystals called magnetosomes that cause the bacteria to orient along geomagnetic field lines (Blakemore 1975). Depending on the species, the bacteria contain either magnetite, $Fe_3O_4$ (Frankel et al. 1979), greigite, $Fe_3S_4$ (Mann et al. 1990; Heywood et al. 1990), or both (Bazylinski et al. 1993a). The bacteria appear to exercise a high degree of control over the sizes, morphologies, and crystallographic orientations of these minerals. Individual magnetosomes are usually arranged in chains, with the easy magnetization axis of the crystals aligned parallel to the chain, providing for the largest possible magnetic dipole moment of the cell (Frankel and Blakemore 1989). A review of magnetotactic bacteria and the magnetic properties of biogenic minerals is given by Bazylinski and Moskowitz (1997).

There is some uncertainty as to which Fe sulfides occur inside the magnetotactic bacteria. Intracellular Fe sulfides are known to be produced by a many-celled, magnetotactic prokaryote (MMP) and several morphological types of single-celled, rod-shaped bacteria (Bazylinski et al. 1994). Only greigite was observed in the rod-shaped species (Heywood et al. 1991), whereas in MMP Mann et al. (1990) found greigite and pyrite ($FeS_2$), and Farina et al. (1990) identified monoclinic pyrrhotite ($Fe_7S_8$). There are no subsequent reports of pyrrhotite, and the presence and role of pyrite in magnetotactic bacteria remains unclear (Bazylinski and Moskowitz 1997). Although information exists about magnetite formation (Frankel et al. 1983; Gorby et al. 1988), nothing has been reported about the mode of formation of greigite in bacteria. In a brief study, we reported that greigite forms by solid-state transformation from mackinawite (tetragonal FeS) (Pósfai et al. 1998); here we discuss our findings in more detail.

The discovery of nanometer-scale magnetite and Fe sulfides in the Martian meteorite ALH84001 and their suggested biogenic origin (McKay et al. 1996) raises the question of whether inorganically formed minerals can be distinguished from those produced by magnetotactic bacteria. Our goals were to identify the Fe sulfide magnetosomes and study their defects and compositions to understand their mechanism of formation and to determine whether the crystals are any different from nonbiogenically formed Fe sulfides. In this study, we present new findings concerning intracellular, bacterially produced Fe sulfides. We discuss microstructural features of magnetite magnetosomes in a companion paper (Devouard et al. 1998).

## EXPERIMENTAL METHODS

Magnetotactic bacteria that produce Fe sulfides only have been described from anaerobic, brackish-to-marine aquatic habitats containing $H_2S$ and have not yet been isolated and cultivated in axenic cultures. We therefore

* Present address: Department of Earth and Environmental Sciences, University of Veszprém, Veszprém, Hungary. E-mail: mposfai@asu.edu

0003–004X/98/1112–1469$05.00

collected cells from natural environments that include a coastal saltwater pond (Salt Pond, Woods Hole, MA, U.S.A.), a series of shallow (<0.5 m deep) salt-marsh pools in the Parker River Wildlife Refuge (Rowley, MA, U.S.A.), and the Sweet Springs Nature Preserve (Morro Bay, CA, U.S.A.).

Salt Pond is a well-characterized, small anaerobic basin that stratifies chemically during the summer months. It is ~5.5 m deep and has marine and freshwater input (Wakeham et al. 1984, 1987). The anaerobic hypolimnion has relatively high concentrations of $H_2S$ (up to 5 m*M*), generated by anaerobic sulfate-reducing bacteria. From April or May to about September, the anaerobic zone rises to within 3 m of the surface, with steep $O_2$ and $H_2S$ gradients. The largest numbers of Fe-sulfide-producing magnetotactic bacteria occur in the anaerobic zone just below the oxic-anoxic interface where $H_2S$ becomes detectable. Water samples from Salt Pond were collected from discrete depths by pumping (Wakeham et al. 1987). Samples were stored at room temperature in glass or polycarbonate bottles that were completely filled to exclude air bubbles.

At the time our samples were collected (summer of 1997), the pH was ~7.4 and the salinity ~29 ppt at the depths from which the samples were drawn. The concentrations of $H_2S$ ranged from 0 to about 900 $\mu M$, as determined by the method of Cline (1969). Concentrations of particulate $Fe^{2+}$ (likely including some magnetosomes) and soluble $Fe^{2+}$ were about 6 $\mu M$ and 5 $\mu M$, respectively, determined as described by Lovley and Phillips (1987).

Samples were collected from the salt-marsh pools by simply filling jars with mud and overlying water, excluding air bubbles as described above. The pH of these samples ranged from 7.2 to 7.8, and the salinity varied from 13 to 32 ppt. $H_2S$ was detected in all samples but its concentration was not determined.

Magnetotactic bacteria were enriched within hours of collection by placing a bar magnet with the south-end next to the side of the jar. Drops from Pasteur pipettes were deposited onto carbon- and Formvar-coated Ni grids for transmission electron microscopy (TEM). The specimens were kept in a grid box in air before and between TEM studies that were performed between a few days and three months after sample collection.

We used a JEOL 2000FX electron microscope operated at a 200 kV accelerating voltage and equipped with a double-tilt (±30°; ±45°) goniometer stage. Particle morphologies and structural defects were observed in TEM images. An ultra-thin-window KEVEX detector was used to study compositions by energy-dispersive X-ray spectrometry (EDS). Pyrite and Cu sulfide standards were used for obtaining experimental k-factors for thin-film analysis. For high-resolution imaging we used a JEOL 4000EX TEM operated at 400-kV accelerating voltage and a 200-kV, Akashi 002B microscope. Fe sulfide structures were identified from single-crystal, selected-area electron diffraction (SAED) patterns that were taken from particles tilted into zone-axis orientations.

The Fe sulfide crystals are enclosed within the cells and could not be extracted by the same methods as the magnetite particles (Devouard et al. 1998). Therefore, the electron beam must travel through amorphous organic material that produces a strong background intensity in the SAED patterns against which the Bragg reflections were commonly difficult to see. The cell contents were also frequently a cause of contamination under the electron beam, which hinders the use of convergent-beam electron diffraction (CBED) and makes high-resolution imaging arduous. The cell may contain some S or Fe outside of the magnetosomes, introducing an unavoidable error into the EDS analyses of magnetosome particles. Despite these problems, TEM can still provide useful information about the Fe sulfide magnetosomes.

## Results

### Types of sulfide-producing organisms and magnetosome morphologies

Both the rod-shaped magnetotactic bacteria and the MMP occurred in the samples from all collecting sites. The MMP consists of 15 to 20 cells that are attached to one another forming a spherical aggregate of cells (Fig. 1a). This organism appears to be a geographically widespread magnetotactic species that is motile as a single unit. Individual cells are only flagellated on their outer sides, providing for the means of motility (Farina et al. 1983; Rodgers et al. 1990). The average number of magnetosome chains within individual cells varies depending on where and when the samples were collected. However, the chains are fairly uniformly distributed among the cells of a given MMP. Most magnetosome chains seem to have a common (E–W) orientation in the exceptionally well-preserved MMP in Figure 1a. In an intact organism the chains are probably aligned parallel to one another. However, the cells commonly disaggregate on the TEM grid (Fig. 2a), and in this case the original chain orientations are not preserved. Most of the single-celled, rod-shaped bacteria contain double or sometimes multiple chains of Fe sulfides (Fig. 3).

The Fe sulfides range from ~30 to ~120 nm in diameter, with most crystals in the 60 to 90 nm range. This observation is consistent with earlier results (Bazylinski et al. 1990) and means that most grains are in the magnetic single-domain size range (Bazylinski and Moskowitz 1997).

In contrast to the well-defined crystal habits of magnetite magnetosomes (Mann et al. 1984; Devouard et al. 1998; see also Figure 3a), most sulfide crystals are subhedral. They are equidimensional or slightly elongated (Fig. 1b), or resemble "barrels" or "egg-timers" in two-dimensional projection. Elongated, arrowhead-shaped greigite crystals occur in some MMPs (Fig. 2b) and rod-shaped bacteria (arrows in Fig. 3b). This morphology has not been previously reported for greigite crystals. Grains with similar morphologies from a variety of magnetotactic microorganisms were all identified as magnetite in

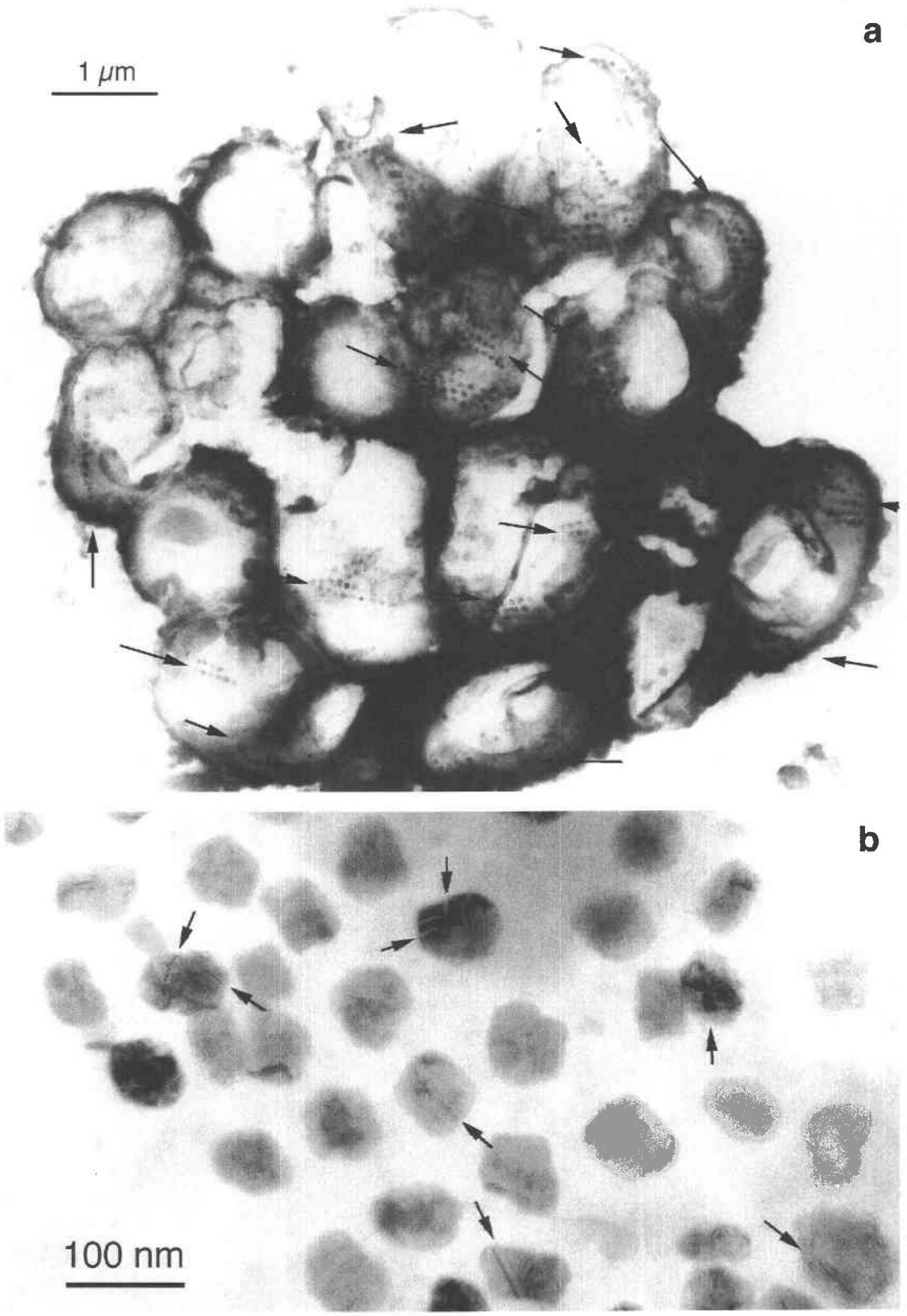


FIGURE 1. (**a**) A well-preserved, many-celled, magnetotactic prokaryote (MMP) from Salt Pond that consists of about 20 individual cells. Fe sulfide magnetosome chains are marked by arrows. (**b**) Fe sulfide magnetosomes from an MMP from Salt Pond. The arrows point to contrast features that indicate structural defects.

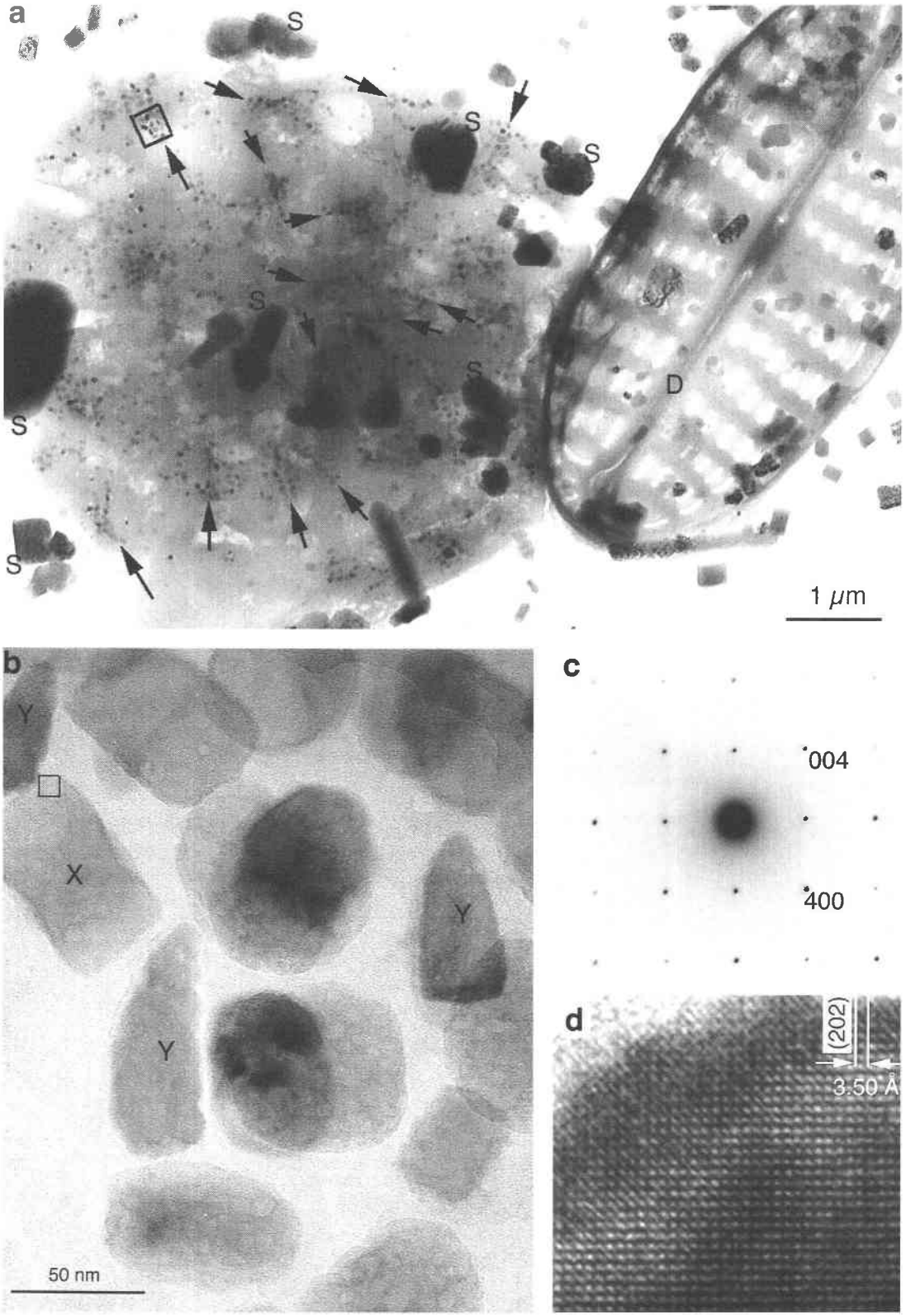


**FIGURE 2.** (**a**) A disaggregated MMP next to a diatom skeleton (D) from Salt Pond. The arrows mark some of the magnetosome chains; S indicates salt (NaCl) crystals resulting from sea water. (**b**) A higher magnification image of the boxed area in **a**, showing greigite crystals with rectangular (X) and arrowhead-shaped (Y) morphologies. (**c**) SAED pattern and (**d**) HRTEM image of crystal X in **b** (all in the corresponding orientations), indicating a well-ordered greigite structure.

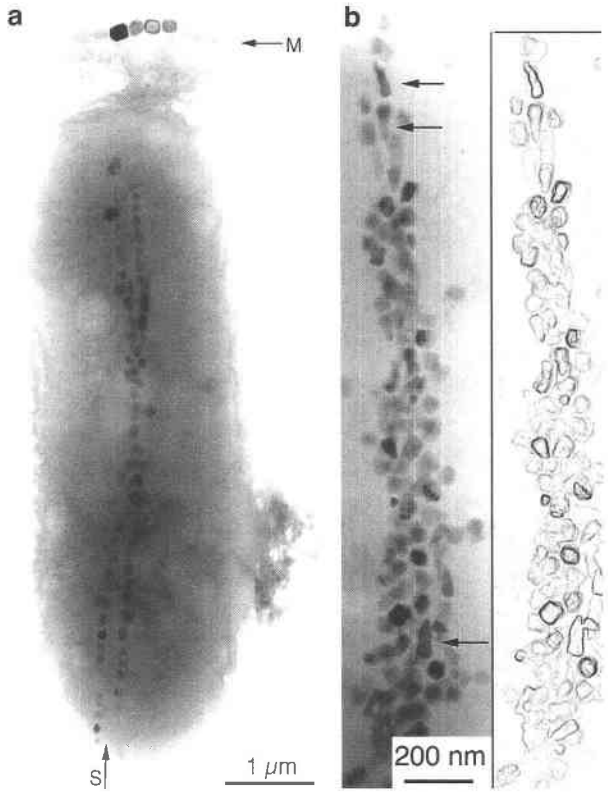


FIGURE 3. Typical rod-shaped, sulfide-producing bacteria. (**a**) A large bacterium from Sweet Springs with a double chain of Fe sulfide magnetosomes (S) attached to a smaller cell that contains only magnetite crystals (M). The magnetite magnetosomes produce more uniform diffraction contrast than the Fe sulfides. (**b**) A multiple chain of sulfide magnetosomes from a rod-shaped bacterium from Salt Pond with many arrowhead-shaped and elongated crystals (arrowed). The right part is a digitally processed version of the TEM image, showing the outlines of the sulfide crystals.

previous studies (Bazylinski et al. 1993a; 1995). In general, the identities of the sulfides seem unrelated to morphologies, and no relationship is obvious between cell types (MMP or rod-shaped) and magnetosome shapes.

### Structures and phase transformations

We identified the structures of about 100 magnetosome crystals from cells of the MMP and rod-shaped bacteria. Our SAED results are summarized and compared to calculated data and published observations in a brief report (Pósfai et al. 1998; Table 1). We found that most magnetosome crystals are greigite in both types of bacteria (see the SAED patterns in Figs. 2c, 4b, and 5b) and that mackinawite (Fig. 4a) can also occur in both types of organisms. A third phase, cubic FeS with the sphalerite structure, was tentatively identified (Pósfai et al. 1998). Neither mackinawite nor cubic FeS had been reported previously from magnetotactic bacteria. None of the magnetosomes from either organism appeared to be pyrite or pyrrhotite.

There is some ambiguity in distinguishing between mackinawite and the presumed cubic FeS magnetosomes on the basis of SAED patterns. Cubic FeS has the sphalerite structure (De Médicis 1970; Takeno et al. 1970); it has not been found in nature, likely because it converts to mackinawite (Murowchick and Barnes 1986; Murowchick 1989; Lennie and Vaughan 1996). The geometries of some of our SAED patterns could be interpreted as different projections of either mackinawite or cubic FeS, and the observed *d*-spacings are intermediate to those of the two structures (Pósfai et al. 1998). However, previous results support the interpretation that some magnetosome crystals are cubic FeS; we believe that the pyrite that was identified by Mann et al. (1990) and Bazylinski et al. (1990) is more likely cubic FeS (Pósfai et al. 1998).

We found that mackinawite within bacterial cells converts to greigite over time (Fig. 4; see also Pósfai et al. 1998). The SAED pattern in Figure 4a was obtained from a mackinawite crystal in a single-celled bacterium less than one week after the specimen was collected. The pattern in Figure 4b was obtained ten days later from the same crystal. The appearance of new reflections along the arrowed reciprocal lattice rows in Figure 4b and the changed *d*-spacings of the remaining ones show that the original mackinawite transformed into greigite. No traces of the mackinawite reflections are observable in Figure 4b, indicating an essentially complete conversion. Horiuchi (1971) observed mackinawite that was coated with amorphous S converting to greigite as a result of prolonged exposure to the electron beam, and Lennie et al. (1997) transformed mackinawite to greigite by heating it in the TEM. Contrary to the results of those studies, we did not observe changes in this crystal (either as mackinawite or as greigite) while it was exposed to the electron beam; instead the transformation occurred during those ten days while the sample was stored between the two studies and shows that mackinawite is a precursor to greigite in these bacteria.

Greigite crystals typically show non-uniform, blotchy diffraction contrast in the electron microscope (Figs. 1b and 5a), a characteristic appearance that can result from thickness variations, lattice strain associated with defects, or the combined effects of both. Greigite crystals commonly contain defects along their (222)-type planes, as also observed by Heywood et al. (1991). Some resemble stacking faults that change the stacking of the close-packed S+Fe layers (Fig. 5c), whereas others seem to be associated with disorder in the Fe distribution, without affecting the S arrangement. We therefore believe that all greigite crystals likely form from a precursor phase (such as mackinawite) by solid-state transformation, and that the planar defects are remnants of the parent structure.

Some magnetosome crystals seem to be in the process of transforming from mackinawite to greigite. Such greigite crystals contain bands parallel to (222) that are several atomic layers thick and have spacings that are consistent with the distance between close-packed layers in mackinawite (Pósfai et al. 1998). The two structures are ori-

**TABLE 1.** EDS analyses (at%) of individual sulfide magnetosome crystals

| Sample | Cell | S | Fe | Cu | (Fe+Cu)/S | Structure | Ref. to figs. |
|---|---|---|---|---|---|---|---|
| SP | MMP | 55.1 | 41.5 | 3.4 | 0.82 | gr | |
| SP | MMP | 55.5 | 42.2 | 2.3 | 0.80 | gr | |
| SP | MMP | 55.0 | 43.1 | 1.9 | 0.82 | gr | |
| SP | MMP | 54.8 | 43.2 | 2.0 | 0.82 | gr | |
| SP | MMP | 57.4 | 42.6 | bl | 0.74 | gr | |
| SP | MMP | 52.1 | 45.7 | 2.1 | 0.92 | ni | |
| SP | MMP | 53.9 | 44.1 | 2.1 | 0.86 | ni | |
| SP | MMP | 55.4 | 41.9 | 2.7 | 0.81 | ni | |
| SP | MMP | 53.9 | 42.1 | 4.0 | 0.86 | ni | |
| SP | MMP | 53.9 | 42.3 | 3.8 | 0.86 | gr | |
| SP | MMP | 52.8 | 42.4 | 4.8 | 0.89 | ni | |
| SP | MMP | 54.0 | 43.1 | 2.9 | 0.85 | ni | |
| SP | MMP | 53.9 | 40.6 | 5.5 | 0.86 | gr | |
| SP | MMP | 51.5 | 44.1 | 4.4 | 0.94 | ni | |
| SP | MMP | 53.9 | 41.5 | 4.6 | 0.86 | gr | |
| | * | 50.0 | 41.9 | 8.1 | 1.00 | | |
| SP | MMP | 52.9 | 43.9 | 3.2 | 0.89 | mk† | B in Fig. 7 |
| | * | 51.8 | 43.6 | 4.6 | 0.93 | | |
| SP | MMP | 52.0 | 42.3 | 5.7 | 0.93 | mk | A in Fig. 7 |
| | * | 50.7 | 39.6 | 9.7 | 0.97 | | |
| SP | MMP | 54.6 | 40.0 | 5.4 | 0.83 | gr | |
| SP | MMP | 45.6 | 44.3 | 10.1 | 1.20 | gr† | C in Fig. 7 |
| SP | MMP | 51.4 | 40.9 | 7.7 | 0.95 | mk/gr† | D in Fig. 7 |
| SP | MMP | 51.6 | 43.0 | 5.4 | 0.94 | gr/mk† | |
| SP | MMP | 51.7 | 44.1 | 4.2 | 0.93 | gr | Fig. 5 |
| SP | MMP | 52.9 | 40.7 | 6.4 | 0.89 | gr | |
| SP | MMP | 53.8 | 41.4 | 4.8 | 0.86 | gr | |
| SP | MMP | 54.0 | 42.9 | 3.1 | 0.85 | gr | |
| SP | MMP | 50.6 | 39.2 | 10.2 | 0.98 | gr | |
| PR | MMP | 60.0 | 40.0 | bl | 0.67 | gr | |
| PR | MMP | 54.0 | 46.0 | bl | 0.85 | gr | |
| PR | MMP | 55.5 | 45.5 | bl | 0.82 | gr | |
| PR | SC | 56.3 | 43.7 | bl | 0.78 | gr | |
| PR | SC | 55.5 | 44.5 | bl | 0.80 | gr | |
| PR | SC | 51.5 | 48.5 | bl | 0.94 | mk | Fig. 4a |
| PR | SC | 53.7 | 46.3 | bl | 0.86 | gr | Fig. 4b |
| SS | SC | 52.7 | 38.2 | 9.1 | 0.90 | gr | |
| SS | SC | 57.4 | 39.4 | 3.2 | 0.74 | gr | |
| SS | SC | 56.4 | 41.2 | 2.4 | 0.77 | gr | |
| SS | SC | 61.0 | 36.7 | 2.3 | 0.64 | gr | |
| SS | SC | 55.2 | 44.8 | bl | 0.81 | gr | |
| SS | SC | 53.9 | 43.9 | 2.2 | 0.86 | gr | |
| SS | SC | 52.5 | 43.7 | 3.8 | 0.90 | gr | |
| SS | SC | 53.5 | 41.0 | 5.5 | 0.87 | gr | |

*Notes:* SP = Salt Pond, MA; PR = Parker River Wildlife Refuge, MA; SS = Sweet Springs Nature Preserve, Morro Bay, CA; MMP = many-celled, magnetotactic prokaryote; SC = single-celled bacterium.

* Duplicate analysis of the same (preceding) magnetosome; bl = below detection limit; gr = greigite; mk = mackinawite; ni = not identified.

† Strongly disordered.

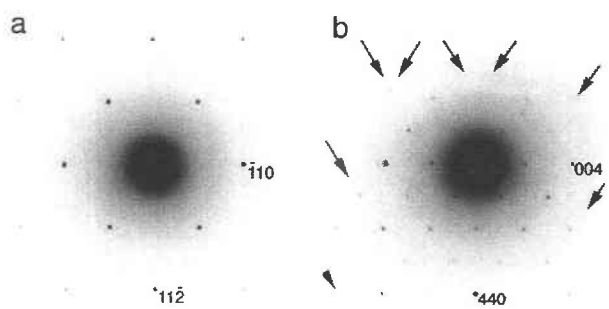


**FIGURE 4.** SAED patterns showing the transformation of (**a**) mackinawite into (**b**) greigite in a rod-shaped bacterium from Parker River. (**b**) Greigite pattern was obtained ten days later than mackinawite. The arrows in **b** mark reciprocal lattice rows containing reflections that are absent in **a**.

ented with respect to one another with $(011)_m//(222)_g$ and $[110]_m//[100]_g$, such that the cubic close-packed S substructure is continuous across the interfaces. The same orientation relationship was observed by Lennie et al. (1997) for mackinawite thermally converted to greigite.

Eight randomly chosen magnetosomes from a rod-shaped bacterium were likely cubic FeS (Fig. 6a), but may have been mackinawite (the problem of distinguishing mackinawite from cubic FeS on the basis of SAED patterns is discussed above). Regardless of whether they are cubic FeS or mackinawite, these crystals are probable precursors to greigite. The HRTEM image (Fig. 6c) of a crystal that seems typical of this magnetosome chain shows a strongly disordered area (marked X) and abundant defects (marked by arrows) along both sets of cubic close-packed planes that are seen edge-on in this orientation. Although the quality of the image does not permit

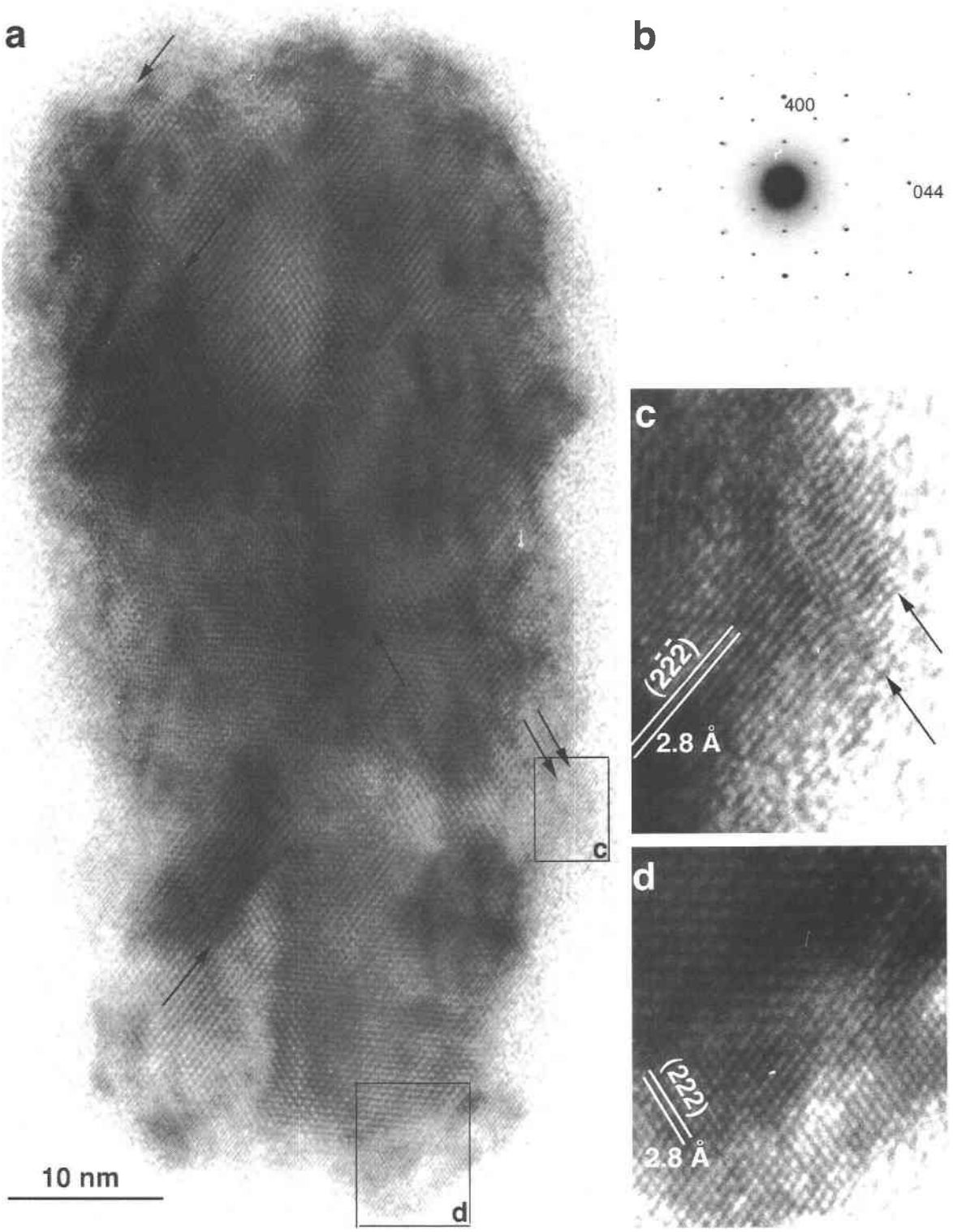


FIGURE 5. (**a**) HRTEM image and (**b**) corresponding SAED pattern of a greigite magnetosome from an MMP from Salt Pond. The arrows in **a** mark planar defects along (222) and (2$\bar{2}$2) planes. Enlargements (**c** and **d**) of the respective boxed regions in **a**, showing two planar faults (arrowed) and an ordered area, respectively.

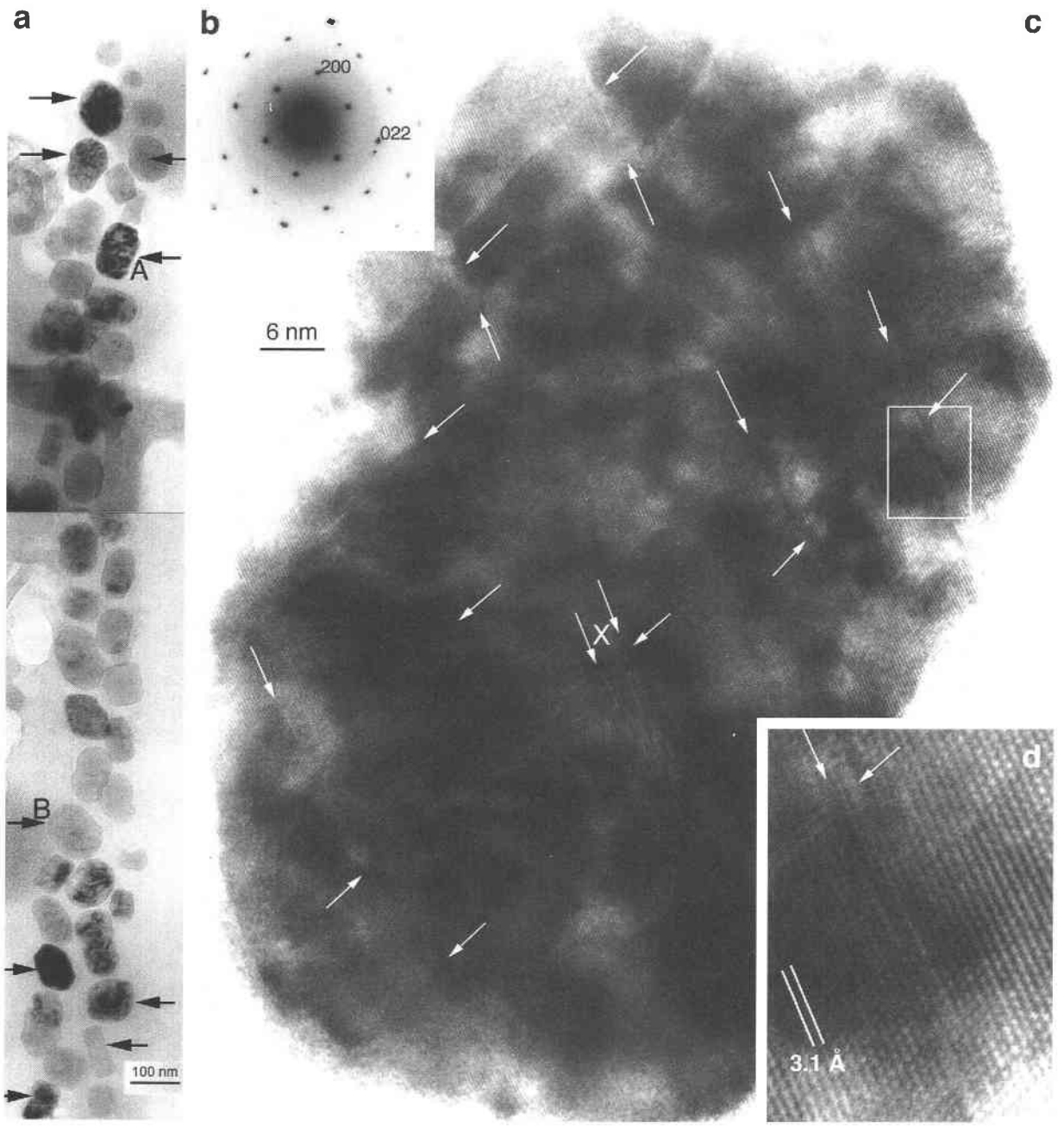


**FIGURE 6.** (**a**) Low-magnification image of a double magnetosome chain from a rod-shaped bacterium from Salt Pond; the arrows mark the randomly chosen crystals from which SAED patterns were obtained. (**b**) SAED pattern and (**c**) HRTEM image of the crystal marked A in **a**; the reflections are indexed according to a sphalerite-type cubic FeS cell. The arrows in **c** mark defects along the close-packed layers, and X marks a disordered area. (**d**) The boxed region, enlarged, shows two planar faults.

the identification of the atomic structure at the defects, we assume that a greigite-like configuration of Fe atoms is present along the defects. If correct, then the crystal in Figure 6c can be regarded as being in the initial stage of transformation (with few atomic layers of greigite in its structure), whereas the crystal in Figure 5 is the end-product of the conversion and contains only a few layers of the precursor structure.

### Positions and orientations of magnetosomes within chains

Mackinawite (Fig. 4a), whether ordered or strongly disordered (Fig. 7a), was found only at the ends of magnetosome chains. Crystals A and B in Figure 7a produced SAED patterns that could be interpreted as mackinawite [001] and [111] projections, respectively. The pattern belonging to A shows additional spots as a result of scat-

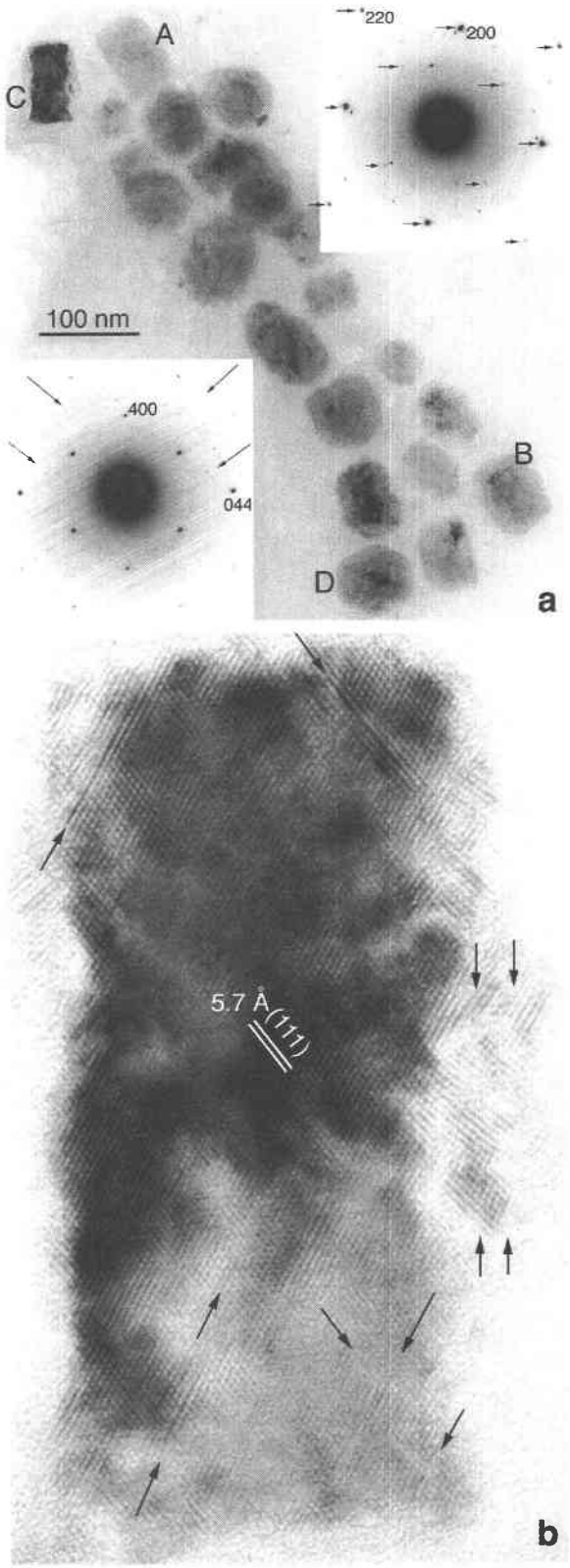


FIGURE 7. (**a**) Fe sulfide magnetosome chain from an MMP from Salt Pond. Crystal A is mackinawite (its SAED pattern is in the upper right), B is poorly ordered mackinawite, C is disordered greigite (its SAED pattern is in the lower left), and D is a heavily disordered crystal. (**b**) HRTEM image of greigite crystal C in **a**, showing defects along (222) and ($2\bar{2}2$) planes (arrowed).
←

tering from other crystals within the TEM selected-area aperture. Diffuse Bragg reflections in the SAED pattern from B (data not shown) indicate that this crystal is poorly ordered and probably a mixture of mackinawite and greigite. Crystal C produced a $[110]_{greigite}$ SAED pattern (lower-left corner in Fig. 7a); however, the faint reflections along the arrowed reciprocal lattice rows suggest that the spinel-type ordering of Fe atoms is not complete (compare this pattern with the one in Fig. 5b). The high-resolution image of the same crystal shows abundant defects along (222)-type planes (arrowed) and patches that are misoriented with respect to the rest of the crystal (marked on the right). Because the chains likely increase in length by the addition of new crystals at the ends (Frankel and Blakemore 1989), the disordered mackinawite (A and B) and greigite (C) crystals are presumably the youngest in the chain and did not completely convert to greigite.

Contrary to the idea that chain formation in bacteria is a magnetism-related physical process (Kirschvink 1990), our observations suggest that the particles are arranged in chains whether or not they are magnetic. The studied crystals within the bacterium in Figure 6 were all mackinawite or cubic FeS, or a mixture of the two, but not greigite. Because mackinawite is diamagnetic (Bertaut et al. 1965) and at room temperature cubic FeS is paramagnetic (Wintenberger et al. 1978), these crystals were aligned in a chain before they had acquired a permanent magnetic dipole moment.

Elongated crystals typically have their long sides approximately parallel to the chain direction. Greigite crystals are preferentially elongated along one of the cube axes and thus aligned with [100] parallel to the chain. This crystallographic orientation was recognized by Heywood et al. (1991) and can also be observed for all greigite images and SAED patterns in this paper (Figs. 2b,c; 5a,b; crystal C in Figs. 7a and b; all SAED patterns are presented in their correct orientations with respect to the corresponding images). Because [100] is likely the easy axis of magnetization in greigite (Bazylinski and Moskowitz 1997), the maximum magnetic moment of the cell is obtained by this preferred orientation of greigite crystals.

The precursor FeS crystals, if elongated, are also aligned with their long sides approximately parallel to the chain (see Fig. 6a). Besides, the crystals are oriented such that when they convert to greigite as described above, then $[100]_{greigite}$ will be parallel to the chain. This orien-

tational relationship is illustrated by the SAED patterns in Figure 6b (in which $200_{\text{cubic FeS}}$ would become $400_{\text{greigite}}$ on conversion) and Figure 7a (by the upper-right pattern, in which $110_{\text{mackinawite}}$ would become $400_{\text{greigite}}$ on conversion).

### Compositions

In addition to Fe and S, most analyzed magnetosomes contain variable Cu up to ~10 at%. Such Cu-bearing magnetosomes were previously described exclusively from the MMP (Bazylinski et al. 1993b); however, we found that both types of bacteria can contain either Cu-free or Cu-bearing sulfide crystals, depending on where the bacteria were collected (Table 1). The sufide magnetosomes from the MMPs or the rod-shaped organisms from Rowley, MA contain no detectable Cu, whereas Cu-bearing Fe sulfide magnetosomes appear typical of bacteria collected from Salt Pond and Morro Bay. Thus, the Cu content likely depends on Cu availability and is independent of the mineral phase. This observation is consistent with our assumption that greigite forms from mackinawite or cubic FeS, because then the Cu content of the precursor phase determines whether the end-product greigite will contain Cu. Mackinawite was reported able to contain up to 8.8 wt% Cu in its structure (Clark 1970), and crystal-chemical considerations suggest that greigite could also contain Cu (Vaughan et al. 1971). Bazylinski et al. (1993b) speculated that bacteria might incorporate Cu into sulfides as a means of detoxification, although the physiological function of Cu in the cell, if one exists, remains unclear.

The Fe(+Cu)/S ratio in most analyzed magnetosomes is higher than 0.75, the value for stoichiometric greigite. Even though our estimated metal/S error can be as high as ±0.1 (for reasons mentioned in the experimental section), and the analysis of Cu seems particularly inaccurate (differences exist in Cu contents between duplicate analyses, Table 1), the excess metal in greigite seems to be significant. When mackinawite or cubic FeS convert to greigite, one fourth of the Fe atoms should be lost. The crystal in Figures 4a and 4b was analyzed before and after the transformation; its composition changed from $Fe_{0.94}S$ to $Fe_{0.86}S$ as it converted from mackinawite to greigite (Table 1). The direction of the change is consistent with the loss of Fe, but the amount lost is less than expected.

A possible sink for the surplus Fe from the mackinawite → greigite conversion could be amorphous nanophase Fe-(OH) that may form when Fe reacts with $O_2$ or $H_2O$ (Lennie et al. 1997). Fe- and O-rich regions surrounding the Fe sulfide magnetosomes were reported by Farina et al. (1990); if such amorphous envelopes exist, they would skew our analyses of greigite crystals toward higher metal/S ratios.

## Discussion

### Formation of sulfide magnetosomes

Greigite and mackinawite were unequivocally identified as mineral phases in the Fe sulfide-producing magnetotactic bacteria. The presence of mackinawite was not previously reported, possibly because it converted to greigite in samples that were stored for more than one or two weeks. The presence of cubic FeS magnetosomes is also likely (Pósfai et al. 1998). The *d*-spacings obtained from the crystals shown in Figure 6 are intermediate between those of cubic FeS and mackinawite and suggest that transitional structures occur, with the Fe atoms partly in mackinawite and partly in sphalerite-type arrangements. Future examination of fresh samples may provide additional information regarding the identities of greigite precursors.

Our data indicate that the bacteria probably do not synthesize greigite crystals directly. Instead, they initially produce either cubic FeS or mackinawite. Our evidence indicates (Fig. 4) that mackinawite magnetosome particles convert to greigite. Other possible transformations that may occur in magnetotactic bacteria include the cubic FeS → mackinawite → greigite and the cubic FeS → greigite series. Similar sequences were also observed in experimental studies of the cubic FeS → mackinawite (Murowchick 1989; Lennie and Vaughan 1996) and mackinawite → greigite conversions (Rickard 1969b; Schoonen and Barnes 1991; Lennie et al. 1997).

All three structures have a cubic close-packed S framework (Fig. 8). The S array can be preserved along the cubic FeS → mackinawite → greigite conversion series, except it slightly contracts as indicated by the decreasing spacings of adjacent close-packed layers. "Mixed" mackinawite/greigite crystals and planar defects along (222)-type planes of greigite indicate that the mackinawite → greigite conversion likely takes place along the close-packed planes through the movement of Fe atoms between neighboring S layers (Pósfai et al. 1998). Disordered structures can result when the transformation is incomplete.

The occurrence of Cu in these sulfides is also notable. There has been interest in whether magnetotactic bacteria are able to incorporate transition metals other than iron into their magnetosomes (Bazylinski and Moskowitz 1997). Clearly, at least the sulfide producers we studied can. The Cu content may have an effect on the rate of conversion to greigite. The crystals in Figure 6 and the disordered mackinawite crystals in Figure 7 did not convert to greigite one month and 2½ months after sample collection, respectively. All these crystals contained Cu (see Table 1), whereas the completely converted crystal in Figure 4 had no detectable Cu.

### Biological significance

Biomineralization of greigite in magnetotactic bacteria resembles the processes of inorganic, sedimentary Fe sulfide formation; in sediments, the amorphous Fe sulfide → (cubic FeS →) mackinawite → greigite transition series is thought to be the main pathway for greigite formation (Morse et al. 1987; Schoonen and Barnes 1991). Greigite then converts to pyrite over time when excess S is present (Berner 1967; Rickard 1969b). Similar transformations

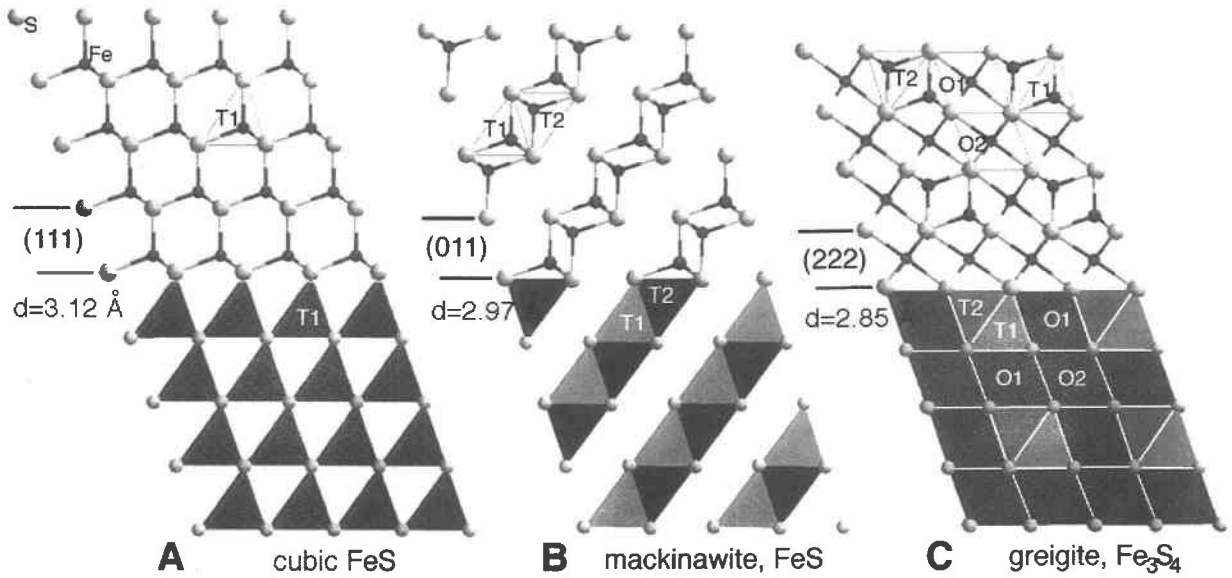


**FIGURE 8.** The structures of (**a**) cubic FeS, (**b**) mackinawite, and (**c**) greigite in [1$\bar{1}$0], [100], and [1$\bar{1}$0] projections, respectively. The upper part of the image shows ball-and-stick models, whereas coordination polyhedra are illustrated in the lower part. The arrangement of S atoms is the same in all three structures, with the cubic-close-packed layers parallel to (111), (011), and (222) in **a**, **b**, and **c**, respectively. In cubic FeS, the Fe atoms completely fill one (marked T1 in **a**) of the two ("up" and "down" oriented) S-tetrahedra that project as isosceles triangles in this projection; in mackinawite, they fill half of both types of tetrahedral sites, marked T1 and T2 (**b**). T1 and T2 are crystallographically equivalent positions; the distinction is made here only to aid visualization. In the spinel-type structure of greigite (**c**), half of all octahedral sites (half of O1 and all O2 positions along the direction of projection) and one-eighth of both T1 and T2 positions are filled.

occur in sulfides that are produced by biologically induced mineralization (BIM); the extracellular conversion of mackinawite to greigite and then to pyrite was observed in batch cultures of *Desulfovibrio desulfuricans,* a dissimilatory sulfate-reducing bacterium (Rickard 1969a).

It is likely that the MMP and other magnetotactic microorganisms that produce Fe sulfide also belong to the group of dissimilatory sulfate-reducing bacteria (DeLong et al. 1993); in addition, these microorganisms exist under conditions where relatively high concentrations of $H_2S$ occur (Bazylinski et al. 1990). Based on the similarities to nonbiogenic and BIM processes of sulfide formation, the greigite particles in cells of magnetotactic bacteria could be expected to convert to pyrite (Bazylinski et al. 1990). However, our results indicate that this final step of the conversion sequence is absent in magnetotactic bacteria. The formation of pyrite from greigite is a slow process (Berner 1970), thus its presence within the relatively fresh bacteria that we studied may not be apparent. On the other hand, truncation of the reaction sequence at greigite appears to make sense in that the further conversion to pyrite would result in the formation of a nonmagnetic phase that is of no use for the bacterium, as far as magnetotaxis is concerned.

Our results also indicate that magnetotactic bacteria synthesize non-magnetic sulfides *de novo,* and align them in chains (as in Figs. 6 and 7) prior to the crystals becoming magnetic. These observations support the idea that the formation of magnetosomes and chain assembly are separately controlled by the bacteria (Bazylinski et al. 1995). The time between two cell divisions is probably not enough for mackinawite to convert to greigite. However, when magnetotactic bacteria divide, their magnetosome chains are presumably divided between the two daughter cells (Blakemore 1982); therefore, these cells inherit crystals that are already ferrimagnetic greigite, imparting the cell with a magnetic dipole moment that is necessary for its magnetotactic response.

## Geological significance

Greigite is an important component of sedimentary Fe sulfides (Morse et al. 1987) and the main carrier of magnetic remanence in many types of young sediments (Hoffmann 1992). Greigite was also reported in soil (Stanjek et al. 1994). In locations where large numbers of magnetotactic bacteria produce Fe sulfides, magnetosome crystals probably contribute to the deposition of greigite in sediments and thus likely to the magnetic remanence. However, given that greigite transforms to pyrite in environments where there is excess S, it is doubtful that greigite would last long in the geologic record (Berner 1967). Thus, the geological significance of bacterial greigite remains unclear.

In principle, the size distributions, morphologies, and microstructural features of greigite magnetosomes might allow bacterial greigite to be distinguished from its non-

biogenic counterparts, although such a distinction is not straightforward. Horiuchi et al. (1974) synthesized greigite crystals with sizes that were approximately in the same range as those in bacteria. In addition, the synthetic crystals contain planar defects parallel to (111)-type planes, as do the bacterially produced grains. The elongated, arrowhead-shaped morphologies of some magnetosome greigite crystals may also not be uniquely characteristic of biogenic greigite. Horiuchi et al. (1974) synthesized needle-shaped greigite from solution at pH 5. These grains were elongated along [110], whereas the long axis of magnetosome crystals is parallel to [100]. Greigite synthesized at pH 9 and 200 °C in the presence of Mn ions typically contained spinel-type twins (Horiuchi et al. 1974). We did not observe such twins in bacterial greigite, although twinning in magnetite magnetosomes appears to be relatively common (Buseck et al. 1997; Devouard et al. 1998).

The occurrence of small (tens of nanometers) pyrrhotite crystals associated with magnetite in the Martian meteorite ALH84001 was cited as evidence of past life on Mars (McKay et al. 1996). We did not identify pyrrhotite in terrestrial magnetotactic bacteria, and so its presence in ALH84001 seems irrelevant to the controversy about past biogenic activity on Mars. Because cubic FeS was found to convert to mackinawite (Murowchick 1989), and our results show that mackinawite converts to greigite within bacteria, these phases are unlikely to persist for long periods and thus be useful as biomarkers. Magnetosome-sized greigite crystals with a narrow size distribution may be the best, although not unambiguous, indicators of the past presence of sulfide-producing magnetotactic bacteria. However, depending on its thermal and chemical environment, greigite can transform into at least three different phases, including smythite (Krupp 1994), pyrrhotite (Skinner 1964), and pyrite (Morse et al. 1987; Schoonen and Barnes 1991). Therefore, with current knowledge the possible bacterial origin of Fe sulfides in terrestrial or extraterrestrial geological samples, such as the Martian meteorite, may be difficult or impossible to prove.

## Acknowledgments

We thank J. Murowchick, B. Moskowitz, I. Dódony, and B. Devouard for helpful discussions and comments, T. Beveridge and J. Banfield for useful reviews, and B. Howes and D. Schlezinger for chemical measurements at Salt Pond. This research was supported by NSF grant CHE 9714101 and NASA grant NAG5-5118. Electron microscopy was performed in the Center for High Resolution Electron Microscopy at Arizona State University.

## References cited

Bazylinski, D.A. and Moskowitz, B.M. (1997) Microbial biomineralization of magnetic iron minerals. In Mineralogical Society of America Reviews in Mineralogy, 35, 181–223.

Bazylinski, D.A., Frankel, R.B., Garratt-Reed, A.J., and Mann, S. (1990) Biomineralization of iron sulfides in magnetotactic bacteria from sulfidic environments. In R.B. Frankel and R.P. Blakemore, Eds., Iron biominerals, p. 239–255. Plenum Press, New York.

Bazylinski, D.A., Heywood, B.R., Mann, S., and Frankel, R.B. (1993a) $Fe_3O_4$ and $Fe_3S_4$ in a bacterium. Nature, 366, 218.

Bazylinski, D.A., Garratt-Reed, A.J., Abedi, A., and Frankel, R.B. (1993b) Copper association with iron sulfide magnetosomes in a magnetotactic bacterium. Archives of Microbiology, 160, 35–42.

Bazylinski, D.A., Garratt-Reed, A.J., and Frankel, R.B. (1994) Electron microscopic studies of magnetosomes in magnetotactic bacteria. Microscopy Research and Technique, 27, 389–401.

Bazylinski, D.A., Frankel, R.B., Heywood, B.R., Mann, S., King, J.W., Donaghay, P.L., and Hanson, A.K. (1995) Controlled biomineralization of magnetite ($Fe_3O_4$) and greigite ($Fe_3S_4$) in a magnetotactic bacterium. Applied and Environmental Microbiology, 61, 3232–3239.

Berner, R.A. (1967) Thermodynamic stability of sedimentary iron sulfides. American Journal of Science, 265, 773–785.

——— (1970) Sedimentary pyrite formation. American Journal of Science, 268, 1–23.

Bertaut, E.F., Burlet, P., and Chappert, J. (1965) On the absence of magnetic order in tetragonal FeS. Solid State Communications, 3, 335–338.

Blakemore, R.P. (1975) Magnetotactic bacteria. Science, 190, 377–379.

——— (1982) Magnetotactic bacteria. Annual Reviews in Microbiology, 36, 217–238.

Buseck, P.R., Devouard, B., Majhi, P., Pósfai, M., Bazylinski, D.A., and Frankel, R.B. (1997) Bacterial magnetite and Fe sulfides. Annual Meeting of the Geological Society of America, Abstracts, A 129. Salt Lake City, Utah.

Clark, A.H. (1970) Nickelian mackinawite from Vlakfontein, Transvaal: A discussion. American Mineralogist, 55, 1802–1807.

Cline, J.D. (1969) Spectrophotometric determination of hydrogen sulfide in natural waters. Limnology and Oceanography, 14, 454–458.

DeLong, E.F., Frankel, R.B., and Bazylinski, D.A. (1993) Multiple evolutionary origins of magnetotaxis in bacteria. Science, 259, 803–806.

De Médicis, R. (1970) Cubic FeS, a metastable iron sulfide. Science, 170, 1191–1192.

Devouard, B., Pósfai, M., Xin, H., Bazylinski, D.A., Frankel, R.B., and Buseck, P.R. (1998) Magnetite from magnetotactic bacteria: Size distributions and twinning. American Mineralogist, 83, 1387–1398.

Farina, M., Lins de Barros, H., Motta de Esquivel, D., and Danon, J. (1983) Ultrastructure of a magnetotactic microorganism. Biology of the Cell, 48, 85–88.

Farina, M., Esquivel, D.M.S., and Lins de Barros, H.G.P. (1990) Magnetic iron-sulphur crystals from a magnetotactic microorganism. Nature, 343, 256–258.

Frankel, R.B. and Blakemore, R.P. (1989) Magnetite and magnetotaxis in microorganisms. Bioelectromagnetics, 10, 223–237.

Frankel, R.B., Blakemore, R.P., and Wolfe, R.S. (1979) Magnetite in freshwater magnetotactic bacteria. Science, 203, 1355–1356.

Frankel, R.B., Papaefthymiou, G.C., Blakemore, R.P., and O'Brien, W. (1983) $Fe_3O_4$ precipitation in magnetotactic bacteria. Biochimica et Biophysica Acta, 763, 147–159.

Gorby, Y.A., Beveridge, T.J., and Blakemore, R.P. (1988) Characterization of the bacterial magnetosome membrane. Journal of Bacteriology, 170, 834–841.

Heywood, B.R., Bazylinski, D.A., Garratt-Reed, A., Mann, S., and Frankel, R.B. (1990) Controlled biosynthesis of greigite ($Fe_3S_4$) in magnetotactic bacteria. Naturwissenschaften, 77, 536–538.

Heywood, B.R., Mann, S., and Frankel, R.B. (1991) Structure, morphology and growth of biogenic greigite ($Fe_3S_4$). Proceedings of the Materials Research Society Symposium, 218, 93–108.

Hoffmann, V. (1992) Greigite ($Fe_3S_4$): Magnetic properties and first domain observations. Physics of the Earth and Planetary Interiors, 70, 288–301.

Horiuchi, S. (1971) Zur Umwandlung von Mackinawit (FeS) in Greigit ($Fe_3S_4$) durch Elektronenstrahlen. Zeitschrift für Anorganische und Allgemeine Chemie, 386, 208–212.

Horiuchi, S., Wada, H., and Moori, T. (1974) Morphology and imperfection of hydrothermaly synthesized greigite ($Fe_3S_4$). Journal of Crystal Growth, 24/25, 624–626.

Kirschvink, J.L. (1990) On the magnetostatic control of crystal orientation and iron accumulation in magnetosomes. Automedica, 14, 257–269.

Krupp, R.E. (1994) Phase relations and phase transformations between the

low-temperature iron sulfides mackinawite, greigite, and smythite. European Journal of Mineralogy, 6, 265–278.

Lennie, A.R. and Vaughan, D.J. (1996) Spectroscopic studies of iron sulfide formation and phase relations at low temperatures. Mineral Spectroscopy: Special Publication No. 5, 117–131.

Lennie, A.R., Redfern, S.A.T., Champness, P.E., Stoddart, C.P., Schofield, P.F., and Vaughan, D.J. (1997) Transformation of mackinawite to greigite: An in situ X-ray powder diffraction and transmission electron microscope study. American Mineralogist, 82, 302–309.

Lovley, D.R. and Phillips, E.J.P. (1987) Rapid assay for microbially reducible ferric iron in aquatic sediments. Applied and Environmental Microbiology, 53, 1536–1540.

Mann, S., Frankel, R.B., and Blakemore, R.P. (1984) Structure, morphology and crystal growth of bacterial magnetite. Nature, 310, 405–407.

Mann, S., Sparks, N.H.C., Frankel, R.B., Bazylinski, D.A., and Jannasch, H.W. (1990) Biomineralization of ferrimagnetic greigite ($Fe_3S_4$) and iron pyrite ($FeS_2$) in a magnetotactic bacterium. Nature, 343, 258–261.

McKay, D.S., Gibson, E.K. Jr., Thomas-Keprta, K.L., Vali, H., Romanek, C.S., Clemett, S.J., Chillier, X.D.F., Maechling, C.R., and Zare, R.N. (1996) Search for past life on Mars: Possible relic biogenic activity in Martian meteorite ALH84001. Science, 273, 924–930.

Morse, J.W., Millero, F.J., Cornwell, J.C., and Rickard, D. (1987) The chemistry of the hydrogen sulfide and iron sulfide systems in natural waters. Earth-Science Reviews, 24, 1–42.

Murowchick, J.B. (1989) Kinetics of the polymorphic transformation of metastable cubic $FeS_{(1-x)}$ to mackinawite (tetragonal $FeS_{(1-x)}$). Geological Society of America Abstracts with Programs, A120.

Murowchick, J.B. and Barnes, H.L. (1986) Formation of cubic FeS. American Mineralogist, 71, 1243–1246.

Pósfai, M., Buseck, P.R., Bazylinski, D.A., and Frankel, R.B. (1998) Reaction sequence of iron sulfide minerals in bacteria and their use as biomarkers. Science, 280, 880–883.

Rickard, D.T. (1969a) The microbiological formation of iron sulphides. Stockholm Contributions in Geology, 20, 50–66.

———(1969b) The chemistry of iron sulphide formation at low temperatures. Stockholm Contributions in Geology, 20, 67–95.

Rodgers, F.G., Blakemore, R.P., Blakemore, N.A., Frankel, R.B., Bazylinski, D.A., Maratea, D., and Rodgers, C. (1990) Intercellular structure in a many-celled magnetotactic prokaryote. Archives of Microbiology, 154, 18–22.

Schoonen, M.A.A. and Barnes, H.L. (1991) Reactions forming pyrite and marcasite from solution: II. Via FeS precursors below 100 °C. Geochimica et Cosmochimica Acta, 55, 1505–1514.

Skinner, B.J., Erd, R.C., and Grimaldi, F.S. (1964) Greigite, the thiospinel of iron; a new mineral. American Mineralogist, 49, 543–555.

Stanjek, H., Fassbinder, J.W.E., Vali, H., Wägele, H., and Graf, W. (1994) Evidence of biogenic greigite (ferrimagnetic $Fe_3S_4$) in soil. European Journal of Soil Science, 45, 97–103.

Takeno, S., Zôka, H., and Niihara, T. (1970) Metastable cubic iron sulfide—with special reference to mackinawite. American Mineralogist, 55, 1639–1649.

Vaughan, D.J., Burns, R.G., and Burns, V.M. (1971) Geochemistry and bonding of thiospinel minerals. Geochimica et Cosmochimica Acta, 35, 365–381.

Wakeham, S.G., Howes, B.L., and Dacey, J.W.H. (1984) Dimethylsulfide in a stratified coastal salt pond. Nature, 310, 770–772.

Wakeham, S.G., Howes, B.L., Dacey, J.W.H., Schwarzenbach, R.P., and Zeyer, J. (1987) Biogeochemistry of dimethylsulfide in a seasonally stratified coastal salt pond. Geochimica et Cosmochimica Acta, 51, 1675–1684.

Wintenberger, M., Srour, B., Meyer, C., Hartmann-Boutron, F., and Gros, Y. (1978) Crystallographic and Mössbauer study of zinc blende type FeS. Journal de Physique, 39, 965–979.

Manuscript received March 20, 1998
Manuscript accepted August 1, 1998
Paper handled by Jillian Banfield